

acetylene is extensively rehybridized when chemisorbed onto group 8 metal surfaces.

**Acknowledgment.** The financial assistance of the Natural Sciences and Engineering Research Council of Canada's Operating, New Ideas and Strategic Energy programs is greatly appreciated. In addition, the generous support of Imperial Oil of Canada, Erindale College, and the Lash Miller Chemical Laboratories is gratefully acknowledged. W.J.P. wishes to thank the NSERC for a postgraduate scholarship. We also wish to thank J. E. Demuth and H. Ibach for a

prepublication communication of their UPS and electron energy loss results for the Ni/C<sub>2</sub>H<sub>2</sub> system.

**Registry No.** <sup>12</sup>C<sub>2</sub>H<sub>2</sub>, 74-86-2; <sup>13</sup>C<sub>2</sub>H<sub>2</sub>, 35121-31-4; Ni(<sup>12</sup>C<sub>2</sub>H<sub>2</sub>), 65583-93-9; Ni(<sup>13</sup>C<sub>2</sub>H<sub>2</sub>), 76900-64-6; Ni(<sup>12</sup>C<sub>2</sub>H<sub>2</sub>)<sub>2</sub>, 76900-65-7; Ni(<sup>13</sup>C<sub>2</sub>H<sub>2</sub>)<sub>2</sub>, 76900-66-8; Cu(<sup>12</sup>C<sub>2</sub>H<sub>2</sub>), 65881-80-3; Cu(<sup>13</sup>C<sub>2</sub>H<sub>2</sub>), 76900-67-9; Cu(<sup>12</sup>C<sub>2</sub>H<sub>2</sub>)<sub>2</sub>, 65881-79-0; Cu(<sup>13</sup>C<sub>2</sub>H<sub>2</sub>)<sub>2</sub>, 76900-68-0; Cu(<sup>12</sup>C<sub>2</sub>H<sub>2</sub>)(<sup>13</sup>C<sub>2</sub>H<sub>2</sub>), 76900-69-1.

**Supplementary Material Available:** Tables VII and VIII, energies, % charges, and partial wave analyses for Ni(C<sub>2</sub>H<sub>2</sub>) and Cu(C<sub>2</sub>H<sub>2</sub>), respectively (10 pages). Ordering information is given on any current masthead page.

Contribution from the Department of Chemistry, University of Calgary, Calgary, Alberta, Canada T2N 1N4, and the Instituto de Fisica e Quimica de Sao Carlos, Universidade de Sao Paulo, 13560 Sao Carlos, Sao Paulo, Brazil

## Molecular Orbital Calculations for the Reaction Fragment NSN

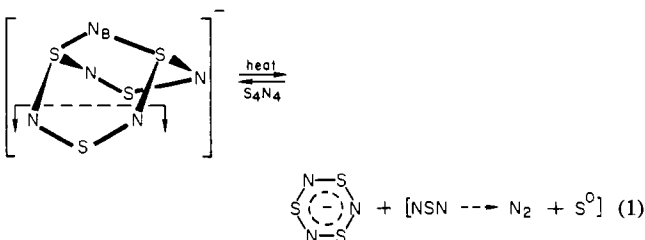
W. G. LAIDLAW\* and M. TRSIC

Received August 6, 1980

An ab initio Hartree-Fock-Slater procedure is employed to reveal local energy minima for two symmetric NSN species NSN90 and NSN180. An additional NSN species leading to a decomposition channel of N<sub>2</sub> + S is also characterized. The linear NNS species is examined for comparison to the symmetric species. These results are discussed in the context of recent experiments on sulfur-nitrogen species.

### Introduction

A number of reactions have recently been discovered<sup>1</sup> which involve the transfer of an NSN fragment to or from a sulfur-nitrogen system as, for example, in the reaction shown in eq 1. This reaction suggests the possibility that the NSN



moiety might be transferred, as such, with a finite mean lifetime. However, attempts to detect this species have not been successful to date.

The only dinitrogen-sulfur species for which there is even tentative claim to experimental characterization<sup>3b</sup> is the N<sub>2</sub>S species for which a linear NNS structure appears to be most favorable.<sup>3a</sup> Nevertheless, since the reaction scheme given in eq 1 involves the cleavage of a symmetrical (linear or bent) NSN structure, one might still wonder whether a metastable NSN species could be involved. Further since the reaction products in these systems are found to be N<sub>2</sub> and elemental sulfur<sup>2</sup> or the oligomer S<sub>8</sub><sup>1</sup>, there is the question of the decomposition channels of any such metastable species.

To explore these possibilities we have employed an ab initio Hartree-Fock-Slater procedure with which we have previously successfully treated nitrogen-sulfur systems.<sup>4</sup> The method utilizes a double- $\zeta$  basis augmented with sulfur d orbitals and invokes a "frozen" core in the manner described by Baerends and Ros.<sup>5</sup> The calculations were of the single determinant spin restricted type, and all species considered were singlets. The total statistical energy was used as a probe of molecular conformation stability.<sup>5</sup> The energy surface for the ar-

angement NSN can be taken to depend on the three variables  $\theta_{\text{NSN}}$ , the angle at S subtended by the nitrogens N<sub>1</sub> and N<sub>2</sub>, and the two "bond" lengths  $R_{\text{SN}_1}$  and  $R_{\text{SN}_2}$ . In the case of the *symmetric* distortions, which we wish to consider,  $R_{\text{SN}_1} \equiv R_{\text{SN}_2}$ , and the problem of finding the energy minimum is reduced to a search in the two variables  $\theta_{\text{NSN}}$  and  $R_{\text{SN}}$ .

For purposes of comparison we carried out our minimization procedure to obtain the most favorable bond lengths for the linear asymmetric species NNS.

### Results

A local minimum in the total statistical energy surface was obtained for  $\theta_{\text{NSN}} = 180^\circ$  and  $R_{\text{SN}} = 1.47 \text{ \AA}$  for the valence electronic configuration  $\sigma_g^4 \sigma_u^4 \pi_g^4 \pi_u^4 (D_{\infty h})$ . We denote this configuration by NSN180, and in Figure 1 we sketch the energy as a function of  $\theta_{\text{NSN}}$  for the optimum distance  $R_{\text{SN}} = 1.47 \text{ \AA}$ . For subsequent reference we give the dependence of this same electronic configuration as a function of  $\theta_{\text{NSN}}$  but for  $R_{\text{SN}} = 1.63 \text{ \AA}$ .

Some 65 kcal above the energy of the NSN180 species we could locate another local minimum near  $\theta_{\text{NSN}} = 90^\circ$  and  $R_{\text{SN}} = 1.63 \text{ \AA}$  with a valence electronic description given by  $a_1^8 a_2^2 b_1^2 b_2^4 (C_{2v})$ . Denoting this case by NSN90 we sketch, in Figure 1, its dependence on  $\theta_{\text{NSN}}$  for the optimum distance  $R_{\text{SN}} = 1.63 \text{ \AA}$ . For subsequent reference we sketch the energy

- (1) (a) T. Chivers and R. T. Oakley, *J. Chem. Soc., Chem. Commun.*, 752 (1979); (b) J. Bojes and T. Chivers, *ibid.*, 453 (1977); *Inorg. Chem.*, **17**, 318 (1978); (c) T. Chivers, R. T. Oakley, A. Wallace, and P. Swepston, *J. Chem. Soc., Chem. Commun.*, 35 (1978); (d) A. Golloch and M. Kuss, *Z. Naturforsch., B: Anorg. Chem., Org. Chem., Biochem., Biophys., Biol.*, **27B**, 1280 (1972).
- (2) The reaction scheme proposed in ref 1c for Ph<sub>3</sub>PN(S<sub>2</sub>N<sub>3</sub>) decomposition to Ph<sub>3</sub>PNSNSS was probed at 10<sup>-6</sup> torr and 100 °C and the vapor, analyzed by photoelectron spectroscopy and quadrupole mass spectrometry, indicated the presence of N<sub>2</sub> and S atoms: N. P. C. Westwood, private communication.
- (3) (a) M. P. S. Collins and B. J. Duke, *J. Chem. Soc., Chem. Commun.*, 277 (1978); (b) F. X. Powell, *Chem. Phys. Lett.*, **33**, 393 (1975).
- (4) (a) J. Bojes, T. Chivers, W. G. Laidlaw, and M. Trsic, *J. Am. Chem. Soc.*, **101**, 4517 (1979); (b) T. Chivers, L. Fielding, W. G. Laidlaw, and M. Trsic, *Inorg. Chem.*, **18**, 3379 (1979); (c) T. Chivers, W. G. Laidlaw, R. T. Oakley, and M. Trsic, *J. Am. Chem. Soc.*, in press.
- (5) (a) E. J. B. Baerends and P. Ros, *Int. J. Quantum Chem., Quantum Chem. Symp.*, No. **12**, 169 (1978); (b) W. G. Laidlaw and M. Trsic, *Chem. Phys.* **36**, 323 (1979).
- (6) W. Flues, O. J. Scherer, J. Weiss, and G. Wolmerhauser, *Angew. Chem., Int. Ed. Engl.*, **15**, 379 (1976).

\* To whom correspondence should be addressed at the University of Calgary.

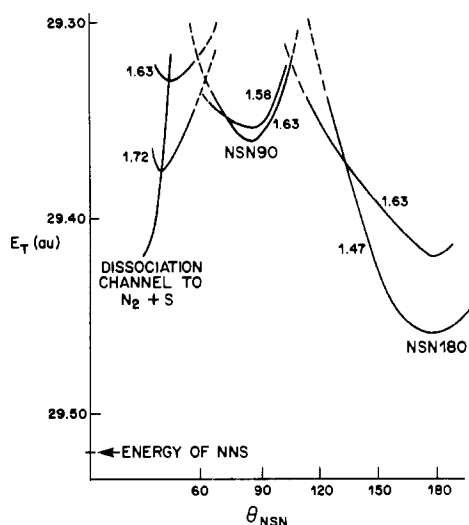


Figure 1. Energy of selected electronic configurations of  $N_2S$  as a function of  $\theta_{NSN}$  and  $R_{SN}$ .

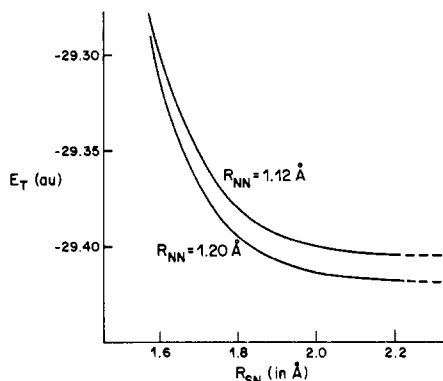


Figure 2. Energy of the electronic configuration  $a_1^8 a_2^0 b_1^4 b_2^4$  in the dissociation channel.

envelope for this configuration as a function of  $\theta$  when  $R_{SN} = 1.58 \text{ \AA}$ .

We can also locate a symmetrical decomposition channel which yields  $N_2 + S$  by following the valence-shell configuration  $a_2^8 a_2^0 b_1^4 b_2^4$  ( $C_{2v}$ ) of NSN. This channel begins in the region of  $\theta_{NSN} = 70^\circ$ , but, as the sketches in Figure 1 indicate, the energy continues to decrease as the distance  $R_{NN}$  is decreased and  $R_{SN}$  increases from 1.63 to 1.72  $\text{\AA}$ , etc. Consequently, a better representation of this channel is to follow the energy of this configuration for fixed  $R_{NN}$  and increasing  $R_{SN} \rightarrow \infty$ . This is displayed in Figure 2 for NN distances of 1.12 and 1.20  $\text{\AA}$ . As expected at sufficiently large  $R_{SN}$  distances (here it is about 2.3  $\text{\AA}$ ), orbitals associated with sulfur become near degenerate (the occupied orbitals  $2b_1$  and  $2b_2$  approach one another and are crossed by the unoccupied  $5a_1$  orbital). Consequently a single determinant representation of this singlet is no longer appropriate.

Further we have been able to confirm the findings of Collins and Duke<sup>3a</sup> that the linear NNS ( $C_{\infty v}$ ) molecule is the lowest energy arrangement for the  $N_2S$  species. Indeed NNS appears to be about 44 kcal below NSN180 with optimized NN and NS distances of 1.16 and 1.63  $\text{\AA}$ , respectively (these compare well to 1.13 and 1.63  $\text{\AA}$  obtained by Collins and Duke).

To better characterize the species indicated above, we provide, in Tables I–III, pertinent information on the orbitals obtained in each case. The species we have denoted by NSN90 has two  $\pi$  symmetry orbitals (four  $\pi$  electrons) which generate an SN overlap population of 0.28 while the  $\sigma$ -type distributions contribute only to 0.13 to the SN overlap population (this small value for  $\sigma$  is a result of the occupation of strongly antibonding

Table I. Orbital Description for NSN90 ( $a_1^8 a_2^2 b_1^2 b_2^4$ ) ( $R_{SN} = 1.63 \text{ \AA}$ )

orbital	eigen-value, $au^a$	character	atom-atom populations <sup>b</sup>			
			N	S	NN	NS
$1a_1$	0.89	$\sigma_{NSN}$	0.15	0.32	0.02	0.09
$1b_2$	0.71	$\sigma_{NS}$	0.35	0.10	-0.03	0.07
$2a_1$	0.51	$\sigma^*_{NS}$	0.23	0.79	0.02	-0.08
$1b_1$	0.37	$\pi_{NS}$	0.11	0.55	0.00	0.05
$3a_1$	0.35	$n_N, n_S$	0.38	0.31	0.00	-0.02
$2b_2$	0.33	$\sigma^*_{NSN}$	0.42	0.34	-0.01	-0.04
$4a_1$	0.25	$n_{SN}, \sigma_{NN}$	0.37	0.21	0.03	0.00
$1a_2$	0.22	$\pi_{NS}, \pi^*_{NN}$	0.46	0.03	-0.02	0.02
$3b_2$	0.19	$\sigma^*_{NN}$	0.52	0.04	-0.08	0.02
$2b_1$	0.14	$\pi^*_{NS}$	0.34	0.58	0.01	-0.07

<sup>a</sup> With opposite signs. <sup>b</sup> Total atom-atom populations for the occupied orbitals: NN, 0.01; NS, 0.41. Charges: N, -0.15; S, 0.30.

Table II. Orbital Description for NSN180 ( $\sigma_g^4 \sigma_u^4 \pi_g^4 \pi_u^4$ ) ( $R_{SN} = 1.47 \text{ \AA}$ )

orbital	eigen-value, $au^a$	character	atom-atom populations <sup>b</sup>		
			N	S	NS
$1\sigma_g$	0.91	$\sigma_{SN}$	0.10	0.44	0.09
$1\sigma_u$	0.81	$\sigma_{SN}$	0.40	0.08	0.04
$2\sigma_g$	0.45	$\sigma^*_{SN}$	0.49	0.52	-0.13
$1\pi_u$	0.39	$\pi_{SN}$	0.12	0.52	0.06
$2\sigma_u$	0.34	$\sigma^*_{SN}$	0.46	0.15	-0.02
$1\pi_g$	0.27	$\pi_{SN}$	0.37	0.06	0.05
$3\sigma_g$	0.16	$\sigma^*_{SN}$	0.29	0.57	-0.04

<sup>a</sup> With opposite signs. <sup>b</sup> Total atom-atom populations for the occupied orbitals: NS, 0.80. Charges: N, -0.21; S, 0.42.

Table III. Orbital Description of Linear NNS ( $\sigma^8 \pi^8$ ) ( $R_{SN} = 1.63 \text{ \AA}, R_{NN} = 1.16 \text{ \AA}$ )

orbital	eigen-value, $au^a$	character	atom-atom populations <sup>b</sup>				
			N	$N_{center}$	S	NN	SN
$1\sigma$	1.04	$\sigma_{NN}$	0.25	0.32	0.02	0.18	0.02
$2\sigma$	0.76	$\sigma_{SN}$	0.06	0.32	0.29	0.01	0.16
$3\sigma$	0.47	$\sigma^*_{NN,SN}$	0.19	0.34	0.82	-0.07	-0.11
$1\pi_x$	0.44	$n$	0.21	0.50	0.03	0.09	0.03
$1\pi_y$	0.44	$n$	0.21	0.50	0.03	0.09	0.03
$4\sigma$	0.39	$\sigma^*_{SN}$	0.99	0.24	0.11	-0.17	-0.01
$2\pi_x$	0.23	$n$	0.24	0.00	0.79	-0.01	0.01
$2\pi_y$	0.23	$n$	0.24	0.00	0.79	-0.01	0.01
$3\pi_{x,y}$	0.09	$\pi^*_{NN}$	0.64	0.57	0.26	-0.20	0.01

<sup>a</sup> With opposite signs. <sup>b</sup> Total overlap population: NN, 0.50; SN, 0.55. Charges: N, -0.03;  $N_{center}$ , 0.02; S, 0.01.

$\sigma$  orbitals). The net overlap population of 0.41 suggests a rather weak single bond.<sup>4</sup> There is very little net NN bonding. In NSN180 the eight  $\pi$  electrons are responsible for all of the net overlap population of 0.81 (the  $\sigma$  antibonding orbitals totally override the  $\sigma$  bonding contributions). The value of 0.81 suggests that this species should be viewed as having almost two full bonds.

The electronic configuration  $a_1^8 a_2^0 b_1^4 b_2^4$  ( $C_{2v}$ ) for NSN in the decomposition channel is characterized by the occupation of the orbital  $2b_1$  which, as the NN distance closes, is the progenitor of a NN  $\pi$  bond. At the same time the  $1a_2$  orbital, which in both NSN90 and NSN180 had had strong  $\pi$ -bonding character for the NS centers, is no longer occupied. Since the net NS bonding in the NSN90 species was about  $2/3\pi$ , this lack of occupancy of  $1a_2$  severely weakens the NS bonding with consequent release of the sulfur species.

For completeness we remark that the linear NNS ( $C_{\infty v}$ ) species with electronic configuration  $\sigma^8 \pi^8$  (see Table III) has

overlap populations of 0.50 and 0.55 for the NN and NS linkages, respectively. This value for the SN overlap suggests a strengthened single bond (cf. to the case of  $S_4N_4$  where the overlap population is 0.49 and the case of  $S_3N_3^-$  where it is 0.52). The charges of -0.027 for the terminal nitrogen, 0.012 for the central nitrogen, and 0.014 for sulfurs are much smaller in magnitude than in any of the symmetric NSN species mentioned above.

### Discussion

The  $S_4N_5^-$  species which has been offered (eq 1) as a possible source of  $N_2S$  has an NSN angle of  $108^\circ$ , an NS bond length of 1.62 Å,<sup>6</sup> and an NS overlap population of 0.38. This is rather similar to the species we have denoted by NSN90 with bond length 1.63 Å and NS overlap population of 0.41. Taking into account the channels sketched in Figure 1, one can estimate a barrier of this species to decomposition of about 9-15 kcal and a barrier for the NSN180 species of about 15-25 kcal.

The transformation of NSN90  $\rightarrow$  NSN180 involves the crossover of electrons from orbital  $4a_1$  to the orbital  $3b_2$ . On the other hand the transformation of NSN90 to the decomposition channel involves the crossover of electrons from orbital  $1a_2$  to the orbital  $2b_1$ . Both one-electron processes would require a perturbation with  $b_2$  symmetry. Thus both of the transformations of NSN90 require the same one-electron perturbation. In the context of the location of NSN in the parent species, e.g., in  $S_4N_5^-$ , this would require that the perturbation be asymmetric with respect to a plane passing through the bridging nitrogen  $N_B$  and the two sulfur atoms below the  $N_4$  plane (cf. eq 1). It is easy to see that  $S_4N_5^-$  or an initial transition state would be symmetric to this symmetry element. Consequently there is some chance that NSN90 could be cleaved intact although the barrier to the decompo-

sition channel is not large. Certainly the experimental work to date<sup>1,2</sup> which yields  $N_2$  and  $S^0$  (or  $S_8$ ) suggests that for cleavage at ca.  $80^\circ\text{C}$  the decomposition channel is readily accessible. However in less vigorous or in constrained environments (e.g., glasses) access to this channel may be more difficult.

Another a priori possibility for the decomposition of NSN is the asymmetrical distortion leading to NS + N products which should themselves be reactive; again we remark that production of  $N_2$  and S in the experiments mentioned above does not seem to favor this path. A further alternative is the asymmetric rearrangement of NSN to the apparently stable NNS. But since NNS has a relatively strong NS bond it would not seem likely that under these conditions linear NNS would be the precursor to the observed  $N_2$  and S decomposition products. We have not probed the channels appropriate to these cases primarily because they are likely to involve a pathway requiring a judicious sequence of variations in all three parameters  $\theta_{SNN}$ ,  $R_{NS}$ , and  $R_{NN}$ .

### Conclusions

Our calculations point to NNS as the lowest energy  $N_2S$  species. Further we have detected two metastable species NSN90 and NSN180 which are in an energy minimum to symmetric variation. For one of these metastable species, NSN90, there is a barrier of roughly 9-15 kcal to decomposition to  $N_2 + S$ .

**Acknowledgment.** The support of NSERC—Canada and FINEP—Brazil operating grants and the award of a Brazil/Canada exchange grant are acknowledged. This work was suggested by T. Chivers and R. T. Oakley and benefitted from discussions with them. Kim Wagstaff's assistance with the calculations is also recognized.

Registry No. NSN, 67200-92-4; NNS, 56400-02-3.

Contribution from the Department of Chemistry and Ames Laboratory—USDOE, Iowa State University, Ames, Iowa 50011

## Synthesis and Spectral Characterization of *fac*- and *mer*-[*N*-(Carboxymethyl)-*L*- $\beta$ -(2-pyridyl)- $\alpha$ -alaninato](*D*-threoninato)cobalt(III), [Co(*N*-Cm-*L*-Pyala)(*D*-Thr)], and the Molecular Structure of the *mer* Isomer

LARRY A. MEISKE, ROBERT A. JACOBSON,\* and ROBERT J. ANGELICI

Received March 26, 1980

Oxidation of Co(II) to Co(III) in the presence of *N*-(carboxymethyl)-*L*- $\beta$ -(2-pyridyl)- $\alpha$ -alaninate (*N*-Cm-*L*-Pyala<sup>2-</sup>) and *D*-threoninate (*D*-Thr<sup>-</sup>) produced two isomers of the complex [Co(*N*-Cm-*L*-Pyala)(*D*-Thr)] which were easily separated on acidic alumina. On the basis of their visible spectra, one isomer was assigned a structure in which the nitrogen atoms are arranged meridionally around the cobalt, while the other was assigned to the only possible facial isomer. Of the three possible meridional isomers, the one isolated was assigned a structure in which the amino nitrogen of the *D*-Thr<sup>-</sup> ligand is coordinated trans to the pyridyl nitrogen of the *N*-Cm-*L*-Pyala<sup>2-</sup> ligand. This assignment was based on the presence of a shoulder on the low-wavelength side of the 537-nm absorption observed in its visible spectrum. This geometry was confirmed by a three-dimensional X-ray analysis of *mer*-[Co(*N*-Cm-*L*-Pyala)(*D*-Thr)] $\cdot\frac{1}{2}$ H<sub>2</sub>O. The compound crystallizes in the monoclinic space group  $P2_1$  with  $a = 10.350$  (4) Å,  $b = 10.339$  (4) Å,  $c = 15.340$  (6) Å,  $\beta = 92.98$  (5) $^\circ$ , and  $Z = 4$ . The structure was solved by the heavy-atom method and refined initially by block-matrix least-squares and finally by full-matrix least-squares procedures to a final weighted  $R$  factor of 0.084. In addition to the crystal structure of *mer*-[Co(*N*-Cm-*L*-Pyala)(*D*-Thr)] $\cdot\frac{1}{2}$ H<sub>2</sub>O, the <sup>1</sup>H NMR, visible, and CD spectra of both the *mer*- and *fac*-[Co(*N*-Cm-*L*-Pyala)(*D*-Thr)] isomers are discussed.

### Introduction

Metal complexes of the two asymmetric tetradentate ligands *N*-(2-pyridylmethyl)-*L*-aspartate (PLASP<sup>2-</sup>) and *N*-(carboxymethyl)-*L*- $\beta$ -(2-pyridyl)- $\alpha$ -alaninate (*N*-Cm-*L*-Pyala<sup>2-</sup>) exhibit

stereoselective effects in coordinating optically active amino acidates (AA<sup>-</sup>).<sup>1,2</sup> Stereoselectivity has also been found in

(1) Nakon, R.; Rechani, P. R.; Angelici, R. J. *Inorg. Chem.* 1973, 12, 2431.